Supplementary information: Conformational and topological correlations in non-frustrated triblock copolymers with homopolymers

Natalie Buchanan, Krysia Browka, Lianna Ketcham, Hillary Le, and Poornima Padmanabhan

Contents

1 Bond Distributions

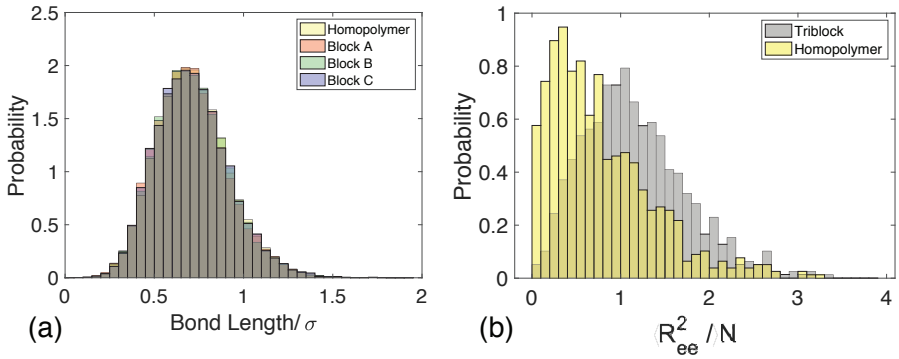

Figure S1: a) Normalized bond distributions comparing the bond lengths in each block from a pure tribock copolymer melt with composition 0.25-0.5-0.25 to the bond lengths in a pure homopolymer melt with a homopolymer chain length of N=60, equal to the full chain length of the triblock copolymer. b) Normalized distribution of the squared end-to-end distance of 0.25-0.5-0.25 triblock copolymers compared against the distribution of the square end-to-end distance for a pure homopolymer melts with homopolymers being the same length as the entire copolymer (N=60)

Since the polymer model used in this study has harmonic bonds, it is possible that the bonds stretch to unphysical lengths. Furthermore, since the Flory-Huggins parameter χ used in this study is relatively high, one might expect that

it causes further bond stretching as the molecule itself spans two interfaces. To verify that neither of these contribute to unphysical stretching, the probability distribution of bond lengths of a pure homopolymer melt and for each block in a triblock ($f_A = 0.25, f_B = 0.5, f_C = 0.25$) are plotted in Figure S1a. The homopolymers are not phase separated, and the contribution of enthalpic bond stretching is not expected to be present. In this case, the distribution reveals that the majority of the bonds are smaller than 1σ and that no unphysical stretching occurs. For the triblock copolymer, phase separation causes a larger end-to-end distance as evidenced in Figure S1b, yet the bond length distribution nearly coincides with the disordered homopolymers. Overall, it can be concluded that the bonds in the triblocks are not stretched, only the polymer conformations are.

2 Equations relating phase diagram variables defined in the main text

The points on the phase diagram in Figure 5a, Figure 6, and Figure 12a are described by ϕ_A, the overall volume fraction of A in the simulation box. The input parameters for the simulations were the mole fraction of added homopolymers (x_h) and the relative length of the homopolymer to that of the A-block in the block copolymer,

$$\alpha = \frac{N_{homopolymer}}{N_{A-block}}. \tag{1}$$

To obtain the overall volume fraction ϕ_A, the fraction of length of the A-block in the copolymer, f_A, is also required. Two block composition compositions were used, $(f_A, f_B, f_C) = (0.25, 0.5, 0.25)$ and $(f_A, f_B, f_C) = (0.2, 0.5, 0.3)$, resulting in $N_{A-block} = 15$ and $N_{A-block} = 12$ respectively. Three different homopolymers with $\alpha = 2/3, \alpha = 1$, and $\alpha = 4/3$ were studied at several values of x_h for the symmetric copolymer. Only one homopolymer chain length $\alpha = 1$ was studied for the asymmetric copolymer.

The overall volume fraction of monomers of type A is given by the ratio of number of beads of type A from both homopolymers and the triblock to the total number of beads in the simulation box.

$$\phi_A = \frac{f_A \alpha x_h + f_A(1 - x_h)}{f_A \alpha x_h + (1 - x_h)} \tag{2}$$

With no added homopolymers (i.e., $x_h = 0$), we get $\phi_A = f_A$.

To correlate the added homopolymer results to the pure triblock melt in Figure 5b, it is necessary to also find ϕ_B, the ratio of number of beads of type B from the triblock to the total number of beads in the simulation box.

$$\phi_B = \frac{f_B(1 - x_h)}{f_A \alpha x_h + (1 - x_h)} \tag{3}$$

Again, with no added homopolymer (i.e., $x_h = 0$), $\phi_B = f_B$. The volume fraction of beads of type C is simply given by

$$\phi_C = 1 - \phi_A - \phi_B. \tag{4}$$

By using a combination of ϕ_A and ϕ_B, the equivalent location of f_A and f_B on the pure triblock melt phase diagram can be found, and the effect of the homopolymer can be found. Values of x_h were chosen so that they followed the same trajectory on the pure triblock phase diagram.

Tanaka *et. al.*[1] reported their results in terms of ϕ_h, the volume fraction of homopolymers, given by

$$\phi_h = \frac{\alpha x_h}{f_A \alpha x_h + (1 - x_h)}, \tag{5}$$

and desribed a correlation for the expansion of the interdomain distance using the equation

$$D/D_0 = 1 + 0.6\phi_h \tag{6}$$

We used Equation 5 to obtain x_h, and compute the corresponding ϕ_A used to make the plot in Figure 8.

3 Phase diagram for ABC copolymer with A-homopolymer

The phase diagram of the **symmetric** triblock copolymer with added homopolymer (Figure 5a) for each box size, homopolymer length, and composition is shown in Table S1. Final morphologies are represented by letters.

The phase diagram of the **asymmetric triblock copolymer** with added homopolymer (Figure 12a) for each box size, homopolymer length, and composition is shown in Table S2. Final morphologies are represented in the phase column by letters.

The structures were identified by counting the number of junctions that meet at each node. Samples for the most prevalent phases are shown in Figure S2.

$\alpha = 2/3$		
ϕ_A	L_{box}/σ	Phase
0.264	25	G
	27	D
	28	D
	31	G
0.28	25	G
	27	D
	28	D
	31	D
0.3	25	G
	27	D
	28	G
	31	N
0.325	25	G
	27	G
	28	D
	31	N
0.357	25	G
	27	G
	28	G
	31	N
0.4	25	G
	27	G
	28	N
	31	N
0.5	25	G
	27	G
0.6	25	N
	27	G

$\alpha = 1$		
ϕ_A	L_{box}/σ	Phase
0.27	25	G
	27	def D
	28	G
	31	D
0.294	25	G
	27	N
	28	N
	31	G
0.323	25	L
	27	N
	28	G
	31	G
0.357	25	N
	27	G
	28	G
	31	G
0.4	25	N
	27	N
	28	G
	31	N
0.437	25	G
	27	G
	28	G
	31	N
0.503	28	G
	31	G
0.602	28	G
	31	G

$\alpha = 4/3$		
ϕ_A	L_{box}/σ	Phase
0.277	25	G
	27	G
	28	D
	31	G
0.308	25	G
	27	G
	28	N
	31	D
0.344	25	G
	27	G
	28	N
	31	P
0.386	25	def PL
	27	G
	28	G
	31	G
0.5	27	G
	28	P
0.6	27	N
	28	G

Table S1: Phase diagram for mixtures of 0.25-0.5-0.25 ABC block copolymer with A-homopolymers at several compositions and box sizes (G = Alternating Gyroid; D = Alternating Diamond; N = Network; L = Lamellar; PL = Perforated Lamellar; P = Plumber's Nightmare; def = Deformed)

$\alpha = 1$		
ϕ_A	L_{box}/σ	Phase
0.272	25	G
	27	G
	28	G
	31	G
0.357	25	G
	27	G
	28	D
	31	D
0.455	25	N
	27	N
	28	G
	31	G

Table S2: Phase diagram for mixtures of 0.2-0.5-0.3 ABC block copolymer with A-homopolymers at several compositions and box sizes (G = Alternating Gyroid; D = Alternating Diamond; N = Network; L = Lamellar; PL = Perforated Lamellar; P = Plumber's Nightmare; def = Deformed)

4 Effect of chain length on domain size

Figure 8 showed that the slope of the curve depends on the ratio of the length of the homopolymer to the A-block, α. In Figure S3 we plot the magnitudes of the slopes in each of the curves shown in Figure 8, and the dependence on α.

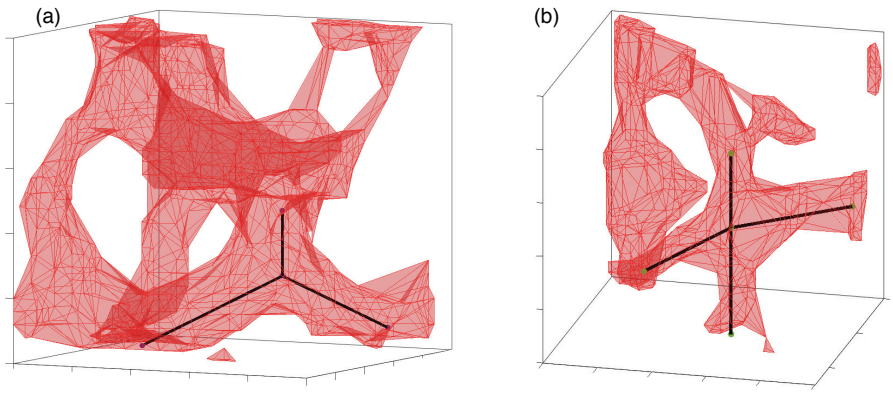

Figure S2: Sample network skeletons to determine symmetry, (a) Gyroid and (b) Diamond.

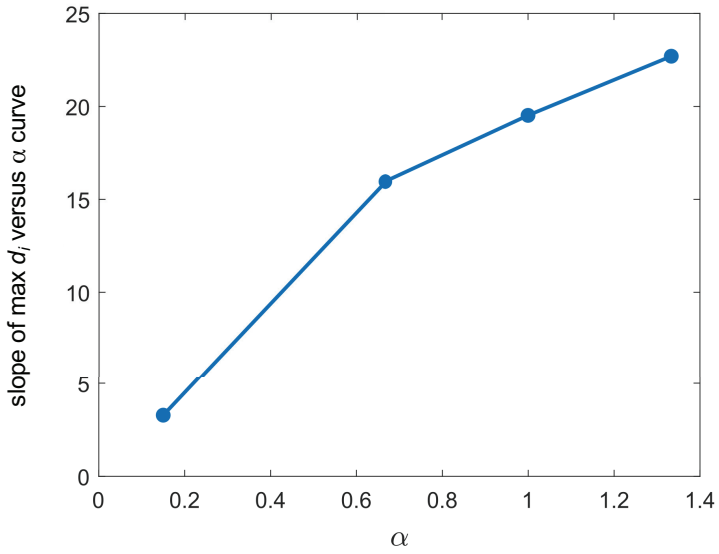

Figure S3: Dependence of domain size slope with chain length of added homopolymer.

5 Histograms of end-to-end distances for each d_i

Figure 11 showed that the $\langle R_{ee}^2 \rangle$ (average value of squared end-to-end distance) increases with d_i for the block copolymer but is flat across d_i for the homopolymer. We can further ask the question whether the distributions themselves, and not just the averages follow a particular trend. The histogram for different R_{ee}^2 (on the x-axis) and each d_i (different colors) are plotted in Figure S4. The top row shows data for the A-block of the block copolymer and the bottom row shows data for the homopolymer. We chose $\phi_A = 0.4$, and two homopolymer lengths ($\alpha = 2/3, 1, 4/3$) for comparison. The relatively high $\phi_A = 0.4$ was chosen so that there are sufficient number of molecules for binning into histograms.

Recall that occupancy for both systems follow similar trends, regardless of α. The blocks from copolymers are primarily located near the interface ($d_i = 1$ and $d_i = 2$). The homopolymers are located deeper in the network. The $\langle R_{ee}^2 \rangle$ were different for both α's. The distributions for the shortest homopolymer, $\alpha = 2/3$, are shown in Figures S4a and S4b. We note that since $\alpha < 1$, the block copolymers tend toward longer end-to-end distances than the homopolymer chains. On the one hand, distribution for the block copolymers changes with distance to the interface. The dependence of $\langle R_{ee}^2 \rangle$ with d_i is reflected in these histograms and the peak shifts to the right with increasing distance from the interface. On the other hand, the distribution for homopolymers is *identical* regardless of d_i.

The distributions for the longest homopolymer, $\alpha = 4/3$, are shown in Fig-

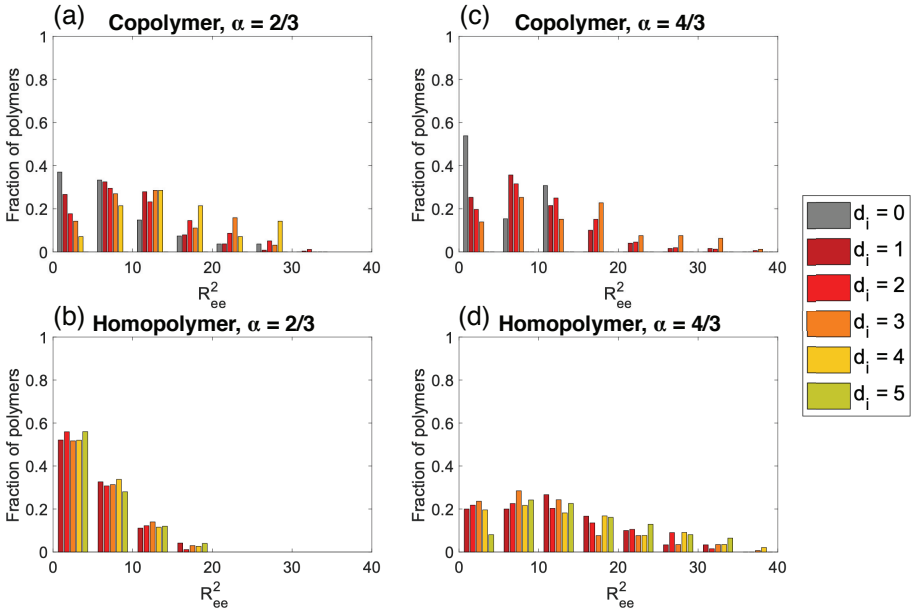

Figure S4: Distribution (not normalized) of end-to-end distances of homopolymers for different d_i for $\phi_A = 0.4$.

ures S4c and S4d. Unlike $\alpha = 2/3$, the blocks and homopolymers both display wider histograms. However, the distributions relate to the distance to the interface in the same manner. For the A-blocks, blocks located at the interface have lower end-to-end distances while those located further away from the interface trend toward longer distances. The homopolymer chains see similar distributions across all d_i's with a peak shifted to the right when compared to the $\alpha = 2/3$ results. The distribution for the longer homopolymer (Figure S4d) appears to be more noisy than that of the shorter homopolymer (Figure S4b), but we believe this arises due to half the number of molecules at the same volume fraction.

Overall, the shapes of the distribution depends on α, but the trend with respect to d_i remains similar. Remarkably, the histograms for the homopolymer appear to be self-similar regardless of distance from the interface, matching the conclusion shown in the main text that $\langle R_{ee}^2 \rangle$ is fairly constant across d_i's.

6 Comparison of end-to-end distances across network-based morphologies

The phase diagram plotted in Figure 5 in the main text shows different morphologies appearing at different box sizes.

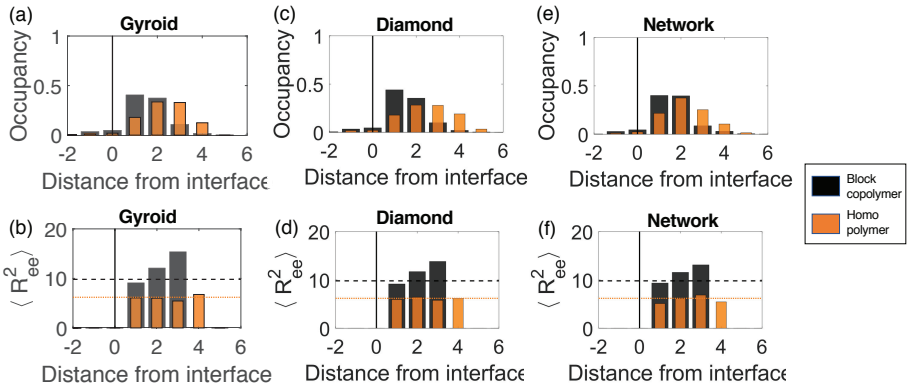

Figure S5: Occupancy and end-to-end distance trends with distance from interface for several network-based morphologies for $\alpha = 2/3$, $\phi_A = 0.3$, and box sizes corresponding to Table S1.

We examined whether the behavior of the end-to-end distances and location of molecules was dependent on the morphology. We compared data from three simulations run at the same point in the phase disgram ($\alpha = 2/3$ and $\phi_A = 0.3$) at different box sizes. Three different morphologies occurred: gyroid, diamond, and network. Figure S5 shows the occupancy in the top row and average end-to-end distance in the bottom row. Similar behaviors are found for all morphologies. The copolymer blocks are located closer to the interface and are more stretched when compared to the homopolymers. The homopolymers are located deeper in the network. Their $\langle R_{ee}^2 \rangle$ is not dependent on d_i and is uniform throughout. The similar distributions suggest that the three morphologies have similar free energies, and nucleate spontaneously in the simulation box.

7 Molecular conformations in lamellar morphologies

For network morphologies formed from the neat triblock copolymer melt, it was found that the A-blocks are located just within the network region. The deeper they are located in the network, the more stretched the block is. To see if this was a phenomenon unique to network morphologies, we also collected conformational data on the lamellar morphologies. The results are shown in Figure S6. The three melts are organized by column. The top row shows the locations (occupancy) of the A-blocks according to the distance from the interface. The bottom row shows the average squared end-to-end distance for each distance to the interface. The data was collected using the method illustrated in Figure 1.

The A-blocks are located deeper in the A-rich region with the majority being located at $d_i = 2$. This results from the linear nature of the lamellar morphology. Network structures have tubes and nodes with various values of d_i

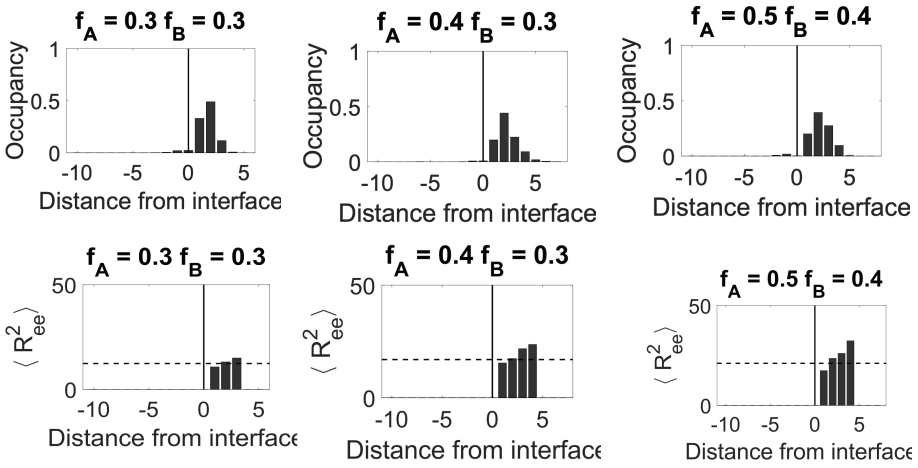

Figure S6: Occupancy and average end-to-end distribution of A-blocks from select three lamellar morphologies that were formed from the neat triblock copolymer melt.

whereas lamellar region are more uniform. The more linear shape of the lamellar regions means that the blocks are more likely to be located at a slightly higher d_i. The sharp boundaries of the lamellar are also reflected in the occupancy distribution with no or very few A-blocks being located outside of the A-rich region.

The average square end-to-end distance increases as d_i increases. The higher d_i means that the center-of-mass of the A-block is located in the center of the A-rich region. Since the block junction is located at the interface of the region, the A-block must be stretched across the region. Therefore, blocks located at higher values of d_i have higher $\langle R_{ee}^2 \rangle$.

References

[1] H. Tanaka, H. Hasegawa and T. Hashimoto, *Macromolecules*, 1991, **24**, 240–251.